

# Geophysical Research Letters<sup>®</sup>



## RESEARCH LETTER

10.1029/2025GL118850

## Change in Tropical Cyclone Efficiency Under Different ENSO Conditions in the Western North Pacific Ocean

Yi-Chun Liao<sup>1</sup> , I.-I. Lin<sup>1</sup> , Jin-Yi Yu<sup>2</sup> , Jia-Yuh Yu<sup>3</sup> , Chun-Chi Lien<sup>1</sup>, and Jui-Yu Chan<sup>4</sup>

<sup>1</sup>Department of Atmospheric Sciences, National Taiwan University, Taipei, Taiwan, <sup>2</sup>Department of Earth System Science, University of California, Irvine, CA, USA, <sup>3</sup>Department of Atmospheric Sciences, National Central University, Taoyuan City, Taiwan, <sup>4</sup>Central Weather Administration, Taipei, Taiwan

### Key Points:

- Sea surface temperature and tropical cyclone (TC) outflow temperature compete to jointly control TC efficiency
- During La Niña, western North Pacific TC efficiency decreases, while during Central Pacific (CP) El Niño, it increases
- Potential intensity (PI) decreases during CP El Niño, but efficiency increases, weakening the decrease in PI

### Supporting Information:

Supporting Information may be found in the online version of this article.

### Correspondence to:

I.-I. Lin,  
[iilin@ntu.edu.tw](mailto:iilin@ntu.edu.tw)

### Citation:

Liao, Y.-C., Lin, I.-I., Yu, J.-Y., Yu, J.-Y., Lien, C.-C., & Chan, J.-Y. (2026). Change in tropical cyclone efficiency under different ENSO conditions in the western North Pacific Ocean. *Geophysical Research Letters*, 53, e2025GL118850. <https://doi.org/10.1029/2025GL118850>

Received 24 AUG 2025

Accepted 14 DEC 2025

**Abstract** Tropical cyclones (TCs) can be considered as Carnot heat engines, where thermodynamic efficiency depends on the sea surface temperature (SST) and TC outflow temperature ( $T_o$ ) in the upper atmosphere. This study investigates how TC efficiency in the western North Pacific (WNP) Ocean varies under different El Niño-Southern Oscillation (ENSO) conditions: the Eastern Pacific (EP), the Central Pacific (CP), and the Mixed El Niño types, as well as La Niña. We also explore how these changes affect a TC's theoretical upper bound (potential intensity (PI)). Using a reanalysis data set from 1979 to 2024, we find that TC efficiency decreases during La Niña, due to warmer  $T_o$ , and increases during CP El Niño, where upper-level cooling dominates. EP and Mixed El Niño show more heterogeneous responses. These efficiency changes contribute to PI variability from  $-38$  to  $+27\%$ , depending on ENSO type and region.

**Plain Language Summary** Tropical cyclones (TCs) are severe natural disasters that are extremely significant in the western North Pacific (WNP), the most active TC basin in the world. WNP TCs are strongly influenced by El Niño-Southern Oscillation (ENSO), and understanding the TC-ENSO relationship is clearly important. In this research, we ask a fundamental question in the WNP TC-ENSO relationship: How does WNP TC efficiency change under different ENSO conditions? The question is based on considering TC as a Carnot heat engine. Our results find an interesting competition between the sea surface temperature (SST) and the TC outflow temperature ( $T_o$ ) in the upper atmosphere in jointly controlling WNP TC efficiency. Because TC efficiency is governed by the difference between SST and  $T_o$ , the higher the SST and the lower the  $T_o$ , the higher the corresponding TC efficiency. In La Niña years, TC efficiency decreases, because even though SST warms, the greater  $T_o$  warming supersedes the contribution of warmer SSTs, leading to a TC efficiency reduction. The reverse is generally found in Central Pacific El Niño years, with mixed results for both the Eastern Pacific and the Mixed El Niño types.

## 1. Introduction

Tropical cyclones (TCs) are severe natural disasters. How TC characteristics may change under different climate conditions is a subject of much interest (e.g., Camargo et al., 2023; Chu & Murakami, 2022; Knutson et al., 2021; Lin et al., 2023; Shields et al., 2020; Sobel et al., 2016, 2021; Wehner & Kossin, 2024; Wing et al., 2015). The western North Pacific (WNP) Ocean is the global ocean basin where the most TCs occur, on average (Schreck et al., 2014). These TCs severely impact the livelihood of the half billion people in the surrounding Asian countries (Peduzzi et al., 2012). The El Niño-Southern Oscillation (ENSO) is the leading tropical mode on interannual timescales and can greatly alter the large-scale atmospheric and ocean environment (e.g., Jin, 1997; McPhaden et al., 2020; Trenberth, 2020). Consequently, understanding how WNP TC characteristics may change under different ENSO conditions is important. Many studies have explored the ENSO-WNP TC relationship (e.g., Camargo et al., 2007; Camargo & Sobel, 2005; Choi et al., 2019; Chu & Murakami, 2022; Ha et al., 2012; Kim et al., 2011; Lee et al., 2025; Lin et al., 2020; Liu et al., 2019; Patricola-DiRosario et al., 2018; Sobel et al., 2023; Song et al., 2020; B. Wang & Chan, 2002; C. Wang et al., 2013; Wu et al., 2018; J. Zhao et al., 2023; H. Zhao & Wang, 2019; Zheng et al., 2015), however, how WNP TC thermodynamic efficiency may change under different ENSO conditions remains an unanswered question.

Emanuel's TC potential intensity (PI) theory (e.g., Bister & Emanuel, 1998; Emanuel, 1986), considers TCs as Carnot heat engines, consisting of two main components: the thermodynamic efficiency and the thermodynamic air-sea disequilibrium (Emanuel et al., 2013; Gilford, 2021; Gilford et al., 2017, 2019; Huan & Yan, 2024; Shields

© 2026. The Author(s).

This is an open access article under the terms of the [Creative Commons Attribution-NonCommercial-NoDerivs License](https://creativecommons.org/licenses/by/4.0/), which permits use and distribution in any medium, provided the original work is properly cited, the use is non-commercial and no modifications or adaptations are made.

et al., 2020; Wing et al., 2015; J. Yu et al., 2010). The thermodynamic air-sea disequilibrium term (hereafter referred to as the energy term) refers to the ocean energy supplied to the TC. This energy term is mainly driven by sea surface temperature (SST) (Emanuel et al., 2013). The thermodynamic efficiency term (hereafter referred to as the efficiency term) is the efficiency of the TC as a heat engine, involving both SST and the TC outflow temperature ( $T_o$ ), with  $T_o$  approximately corresponding to the environmental temperature near the tropopause (Emanuel & Rotunno, 2011). Given this heat engine framework, how the efficiency term may change under different environmental conditions is thus highly intriguing, especially in the context of the ENSO-WNP TC relationship.

ENSO exhibits considerable complexity beyond a simple El Niño–La Niña dichotomy (Capotondi et al., 2020; Timmermann et al., 2018), with distinct types of El Niño potentially exerting varied impacts on atmospheric and oceanic environments of the WNP. Notably, ENSO events can be classified into Eastern Pacific (EP) and Central Pacific (CP) types based on the location of maximum SST anomalies (Ashok et al., 2007; Kao & Yu, 2009; Kug et al., 2009). EP El Niño features peak warming in the eastern equatorial Pacific, often producing stronger upper-tropospheric warming due to enhanced deep convection in that region. In contrast, CP El Niño has SST anomalies centered farther west, near the dateline, leading to different convective and atmospheric heating patterns. More recently, a Mixed type (Mix) of El Niño has been identified, characterized by warming in both central and eastern Pacific regions and exhibiting hybrid dynamical responses (Paek et al., 2017; J.-Y. Yu & Kim, 2013). These ENSO types influence not only SST patterns relevant to the energy input to TCs but also the vertical thermal structure of the atmosphere (Chiang & Sobel, 2002; Trenberth et al., 2002). Here we explore how TC efficiency may change under different ENSO conditions. The scientific goals of this research are to: (a) explore changes of heat engine efficiency under different ENSO conditions for WNP TCs, and (b) explore how this change in heat engine efficiency may contribute to PI changes of WNP TCs for different ENSO conditions.

## 2. Data and Methodology

This study focuses on the WNP TC Main Development Region (MDR; 120°–180°E, 10°–25°N) over the period 1979–2024. We use monthly data with a 0.25° resolution from the European Centre for Medium-Range Weather Forecasts fifth-generation reanalysis (ERA5; Hersbach et al., 2020).

The classification of ENSO is based on the average from August to November (ASON) of the ENSO development year. The period is chosen to capture the influence of the ENSO signal on TCs as they are closer to the mature phase of ENSO. Additionally, based on the U.S. Joint Typhoon Warning Center best-track archive data from 1979 to 2024, TCs that occur in the WNP between August and November account for ~66% of the annual total. El Niño and La Niña events are determined by the monthly Niño-3.4 index obtained from the National Oceanic and Atmospheric Administration Climate Prediction Center website at: [https://www.cpc.ncep.noaa.gov/products/analysis\\_monitoring/ensostuff/ONI\\_change.shtml](https://www.cpc.ncep.noaa.gov/products/analysis_monitoring/ensostuff/ONI_change.shtml). Years with an ASON Niño-3.4 index >0.5 (<-0.5) are categorized as El Niño (La Niña) years, while those in between are classified as Neutral (i.e., normal years). El Niño events are further divided into EP, CP, and Mix types based on the EP and CP index obtained from <https://www.ess.uci.edu/~yu/2OSC/> (Kao & Yu, 2009; J.-Y. Yu & Kim, 2010). An El Niño event is classified as an EP type when the EP index exceeds the CP index by more than 0.5, as a CP type when the CP index exceeds the EP index by more than 0.5, and as a Mix type when the difference between the two indices is 0.5 or less. The ENSO years assigned to each category are listed in Table S1 in Supporting Information S1.

To isolate ENSO-related variations from long-term climate trends, a least-squares linear detrending is applied to all variables. This ensures that differences between ENSO and Neutral years reflect interannual variability rather than long-term climate change. Statistical significance ( $p < 0.05$ ) is assessed using the Wilcoxon-Mann-Whitney test, a classic non-parametric test. This approach has the advantage that it does not need to assume that the samples follow a Gaussian distribution (Chu, 2002; Hsu et al., 2014; Wilks, 2019). In addition, because we only have three cases for the EP and the Mix El Niño, there is an under-sampling issue. To address this and improve the statistical robustness, we use a 1° × 1° window method to conduct our sampling. Because the original grid size is 0.25°, we have 16 samples within each 1° × 1° window. The statistical test is thus based on this 1° × 1° window. For Figures 1 and 3 (spatial distribution), a statistical test was performed for each 1° × 1° window to represent the test result within that area. For Figure 2 and Table 1 (MDR average results), to maintain consistency in our statistical calculations, the average value within each 1° × 1° area is used as a sample.

TC thermodynamic efficiency is derived from PI theory. Here we express PI (e.g., Bister & Emanuel, 1998) as:

$$PI^2 = \frac{C_k}{C_d} \frac{SST - T_o}{T_o} (k_o^* - k) \quad (1)$$

where SST is the pre-cyclone sea surface temperature,  $T_o$  is the TC outflow temperature,  $k_o^*$  is the saturation enthalpy at the sea surface,  $k$  is the air enthalpy near the surface, and  $C_k$  and  $C_d$  are the enthalpy exchange and drag coefficients, respectively.

To assess how the efficiency affects changes in PI, we take the natural logarithm of Equation 1 following previous studies (e.g., Emanuel et al., 2013; Shields et al., 2020; Wing et al., 2015):

$$2 \ln PI = \ln \frac{C_k}{C_d} + \ln \frac{SST - T_o}{T_o} + \ln(k_o^* - k) \quad (2)$$

In this study, we use  $\ln\left(\frac{SST - T_o}{T_o}\right)$  as the efficiency term and  $\ln(k_o^* - k)$  as the energy term. Following Wing et al. (2015), we calculate PI using the algorithm of Bister and Emanuel (2002) rather than computing Equation 1 directly.  $T_o$  is derived from the Bister and Emanuel (2002) algorithm instead of the temperature at a fixed height. The ratio of  $\frac{C_k}{C_d}$  is set to a constant value of 0.9. The energy term is the residual of the remaining terms in Equation 2 (Wing et al., 2015). We compute the fractional change of efficiency and energy relative to the change in PI, and express the result in the same units (m/s) to assess their contributions. The statistical analyses for the efficiency and energy terms after unit conversions are presented using  $\ln\left(\frac{SST - T_o}{T_o}\right)$  and  $\ln(k_o^* - k)$  in Equation 2.

### 3. Results

#### 3.1. Changes in TC Thermodynamic Efficiency Under Different ENSO Conditions

As mentioned earlier, El Niño events are classified into three types: EP, CP, and Mix. Together with La Niña, we identify four types of ENSO events. TC thermodynamic efficiency under each of these conditions is compared against Neutral conditions. The results are illustrated in Figures 1 and 2.

We find significant thermodynamic efficiency changes under different ENSO conditions (Figure 1). Relative to neutral ENSO, TC thermodynamic efficiency in the MDR decreases during La Niña (Figure 1a). According to Equations 1 and 2, efficiency depends on the temperature difference between SST and  $T_o$  (i.e.,  $SST - T_o$ ). During La Niña, the WNP warm pool shifts westward, resulting in positive SST anomalies in the western WNP (Chu & Murakami, 2022; McPhaden et al., 2020). In the western MDR (120°–150°E, 10°–25°N), the rise in SST favors efficiency increases. However,  $T_o$  also increases which acts to decrease efficiency. Because the increase in  $T_o$  exceeds the increase in SST, the term  $SST - T_o$  has a negative anomaly under La Niña, therefore reducing TC efficiency. In the eastern MDR (150°–180°E, 10°–25°N), SST decreases and  $T_o$  increases, further reducing  $SST - T_o$  and leading to decreased efficiency.

EP El Niño conditions (Figure 1b) result in SST decreases across the WNP (Kug et al., 2009), while changes in  $T_o$  are spatially heterogeneous. In the western MDR,  $T_o$  has a positive anomaly.  $SST - T_o$  is generally negative, indicating decreased efficiency. In the eastern MDR,  $T_o$  has a negative anomaly that exceeds the SST decrease, leading to a positive  $SST - T_o$  anomaly and increased efficiency. For CP El Niño (Figure 1c), SST also anomalously decreases, but  $T_o$  decreases more substantially. The resulting increase in  $SST - T_o$  leads to enhanced efficiency across both MDR regions, with the eastern MDR experiencing a stronger increase. During Mix El Niño events (Figure 1d), the pattern is similar to EP El Niño. Although SST shows slight positive anomalies near land, a marked positive anomaly in  $T_o$  leads to a negative  $SST - T_o$ , reducing efficiency in the western MDR.

Figure 2 summarizes the average efficiency for each ENSO type in the western and eastern MDR. Some regional averages differ from the overall patterns in Figure 1, reflecting the coexistence of positive and negative anomalies within each region (e.g., the western MDR during Mix El Niño). Overall, TC thermodynamic efficiency tends to decrease during La Niña, increase during CP El Niño, and shows mixed signals under the EP and Mix type. These variations are largely governed by the  $SST - T_o$  difference, with  $T_o$  playing a particularly influential role. Given these efficiency changes, we next explore how these changes may contribute to changes in PI.

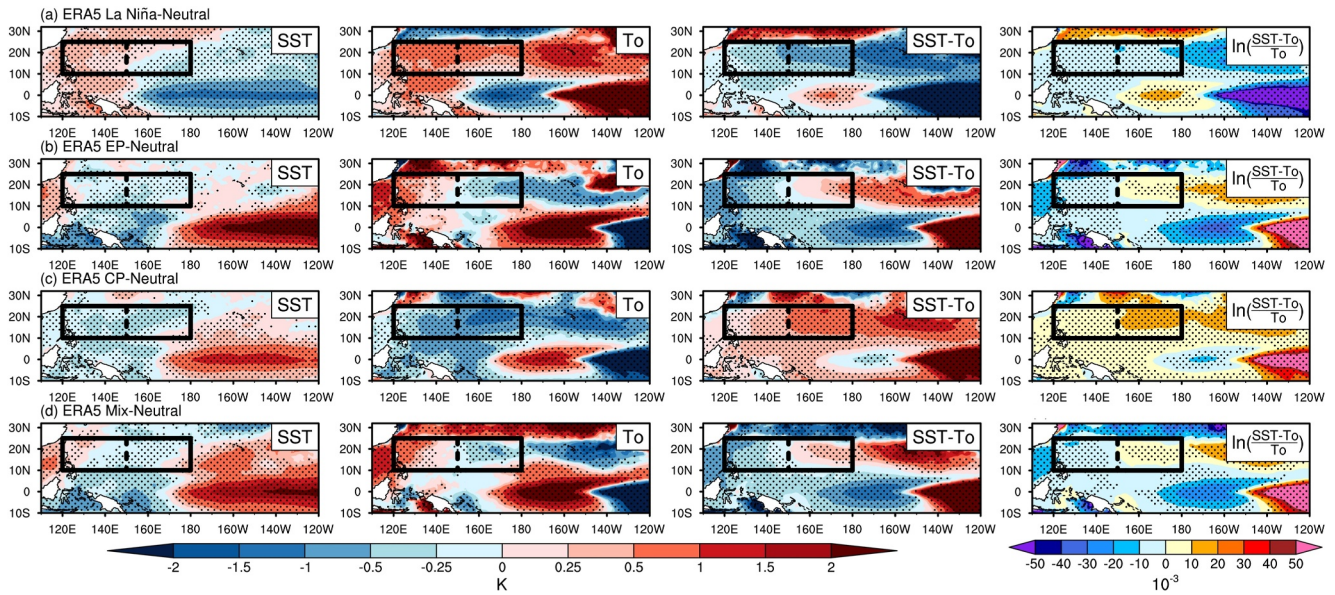


**Figure 1.** Spatial distribution of sea surface temperature (SST),  $T_o$ ,  $SST-T_o$ , and efficiency ( $\ln(\frac{SST-T_o}{T_o})$ ) terms for (a) La Niña, (b) Eastern Pacific (EP) El Niño, (c) Central Pacific (CP) El Niño, and (d) Mix El Niño minus neutral El Niño-Southern Oscillation from ERA5. The black boxes indicate the MDR. The 150°E longitude denoted by the dashed line divides the MDR box into two areas. The areas with black dots indicate statistical significance. The figure is displayed based on a  $1^\circ \times 1^\circ$  spatial resolution.

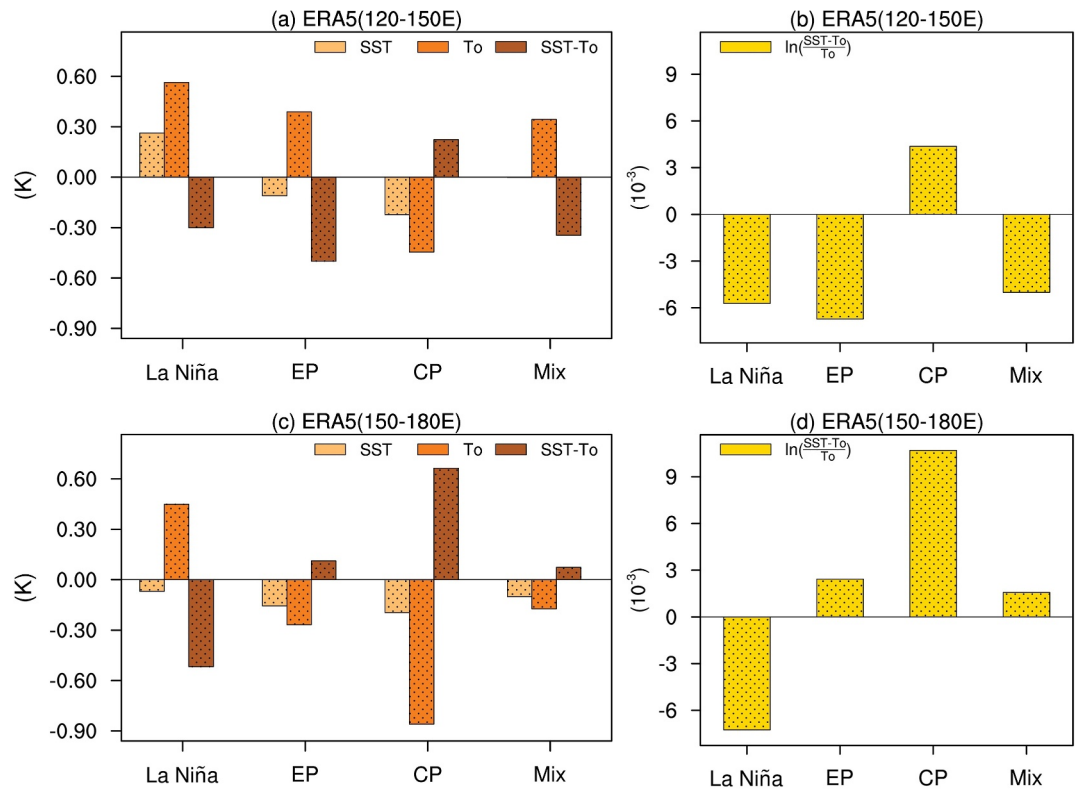


**Figure 2.** Western MDR average (120°–150°E, 10°–25°N) (a) sea surface temperature (SST),  $T_o$ , and  $SST-T_o$ , and (b) efficiency ( $\ln(\frac{SST-T_o}{T_o})$ ) for different types of El Niño-Southern Oscillation (ENSO) minus neutral ENSO, based on ERA5 data. (c) and (d) as in (a) and (b), but for the eastern MDR (150°–180°E, 10°–25°N). Each bar chart with a stipple fill pattern shows statistical significance.

### 3.2. Contribution of Changes in TC Thermodynamic Efficiency to PI Under Different ENSO Conditions

As we have previously discussed, PI consists of 2 terms: the efficiency term and the energy term. Using the decomposition method described in Section 2, we evaluate the relative contributions of these terms to PI under different ENSO conditions.

We begin with La Niña. As shown in Figure 1a (and also in Figure 3a), thermodynamic efficiency decreases (e.g., negative anomaly compared with Neutral). This in itself is a negative contribution to the change in PI. Nevertheless, within the western MDR, we find positive PI anomalies. This is because in this region the energy term is a larger contributor than is the efficiency term. During La Niña years, we find positive SST anomalies in the western MDR (Figure 1a), resulting in a positive contribution from the energy term that outweighs the negative impact of reduced efficiency. As summarized in Table 1, PI increases by 1.88 m/s compared with Neutral years, with the energy term contributing +2.09 m/s and the efficiency term contributing  $-0.21$  m/s. In other words, of the total PI anomaly of 1.88 m/s (i.e., 100%), the equivalent positive contribution of the energy term is +111% while the negative contribution from efficiency is  $-11\%$ . In contrast, in the eastern MDR, PI decreases by  $-0.75$  m/s. This negative anomaly is partly due to a negative contribution from the efficiency term ( $-38\%$ ) and a more significant impact from the energy term ( $-62\%$ ), which is linked to decreased SST.

For the three El Niño types, we begin with EP El Niño. As shown in Figure 3b and Table 1, we find anomalously negative PI over the WNP. This reduction is associated with decreased SST in the WNP (Figure 1b), since warm waters shift toward the central and eastern Pacific and the WNP warm pool weakens, given the relaxed trade winds (Chu & Murakami, 2022; McPhaden et al., 2020). In the western MDR, both the efficiency and energy terms contribute to the negative PI anomaly. While both terms are statistically significant contributors (Table 1), the energy term is a larger contributor ( $-74\%$ ) than the efficiency term ( $-26\%$ ). In the eastern MDR, the efficiency term provides a small positive contribution of  $+0.1$  m/s (8%), while the energy term contributes  $-1.35$  m/s ( $-108\%$ ). For CP El Niño (Figure 3c and Table 1), PI is also anomalously negative. However, unlike EP events,

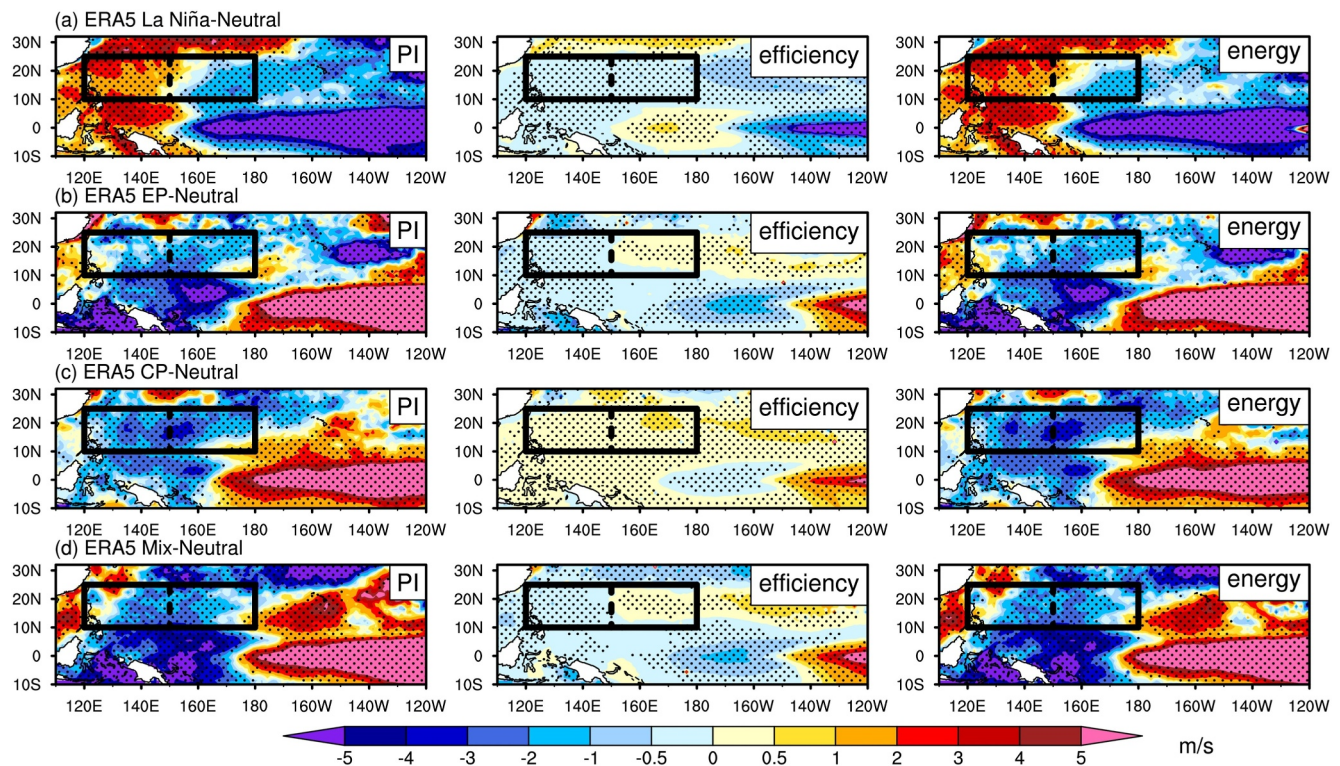


**Figure 3.** Spatial distribution of potential intensity (PI, left), efficiency (middle), and energy (right) terms for (a) La Niña, (b) Eastern Pacific (EP) El Niño, (c) Central Pacific (CP) El Niño, and (d) Mix El Niño minus neutral El Niño-Southern Oscillation from ERA5 (shaded; m/s). The black boxes indicate the MDR. The 150°E longitude denoted by the dashed line divides the MDR box into two areas. The areas with black dots indicate statistical significance. The figure is displayed based on a  $1^\circ \times 1^\circ$  spatial resolution.

**Table 1**

Mean PI, Efficiency, and Energy Terms for Different Types of ENSO Minus Neutral ENSO Over the Western and Eastern of the MDR From ERA5

Types	PI (m/s) (Contribution percentage for PI, %)	Contribution from efficiency (m/s) (Contribution percentage for PI, %)	Contribution from energy (m/s) (Contribution percentage for PI, %)
Western MDR (120°–150°E, 10°–25°N)			
La Niña	1.88 (100%)	−0.21 (−11%)	2.09 (111%)
EP El Niño	−0.99 (−100%)	−0.26 (−26%)	−0.73 (−74%)
CP El Niño	−1.67 (−100%)	0.16 (10%)	−1.83 (−110%)
Mix El Niño	−1.11 (−100%)	−0.20 (−18%)	−0.91 (−82%)
Eastern MDR (150°–180°E, 10°–25°N)			
La Niña	−0.75 (−100%)	−0.28 (−38%)	−0.47 (−62%)
EP El Niño	−1.26 (−100%)	0.10 (8%)	−1.35 (−108%)
CP El Niño	−1.52 (−100%)	0.41 (27%)	−1.93 (−127%)
Mix El Niño	−1.42 (−100%)	0.06 (4%)	−1.48 (−104%)

Note. All values have statistical significance. The contribution percentage for PI is obtained by dividing by the average PI amplitude.

efficiency increases during CP events (as discussed in the previous section), contributing +10% in the western MDR and +27% in the eastern MDR. These increases in efficiency partially offset the negative contributions from the energy term, which account for −110% and −127% in the western and eastern MDR, respectively. In other words, the increase in the efficiency term during CP El Niño helps to reduce the net decrease in PI caused by the energy term. For the Mix El Niño (Figure 3d and Table 1), the results are similar to the EP El Niño, with PI decreases primarily driven by the energy term.

#### 4. Discussion and Conclusion

The WNP on average is the largest generator of TC activity in the world, and ENSO is a leading climate mode influencing WNP TCs. Though there have been numerous studies conducted in understanding the WNP TC-ENSO relationship, how WNP TC thermodynamic efficiency may be influenced by ENSO is an intriguing and fundamental question which has not been thoroughly investigated. This new research contributes to narrowing this knowledge gap. We find that the interplay between SST and TC outflow temperature ( $T_o$ ) jointly controls TC thermodynamic efficiency under different ENSO conditions (La Niña, EP, CP, and Mix El Niño).

During La Niña years, thermodynamic efficiency decreases. This is because even though SST increase, the  $T_o$  increases even more. During El Niño, thermodynamic efficiency increases during CP El Niño, primarily due to a significant decrease in  $T_o$  that exceeds the corresponding SST cooling. For EP and Mix El Niño conditions, SST anomalies are mostly negative in MDR, but  $T_o$  displays a more diverse pattern. Thus, the efficiency term signal varies between the western and eastern MDR. Those changes in efficiency contribute −38% to +27% to the change in PI, depending on the ENSO type and region.

The above discussion starts from the perspective of thermodynamic efficiency. Another way to view the results is to start from the PI change perspective. The energy term is a larger control on PI than is the efficiency term. Therefore, the sign of PI follows the sign of the energy term. In the western MDR during La Niña, due to an increase in the energy term (primarily due to the SST increase), PI increases. During La Niña, the efficiency term decreases, opposing the contribution by the energy term. Because the efficiency term is a smaller term, it weakens PI increase due to the energy term. More quantitatively, the average PI increases by 1.88 m/s, with the positive contribution from the energy term being 2.09 m/s, and the negative contribution from the efficiency term being −0.21 m/s. Similarly, for CP El Niño, because the energy term decreases (since SST cools over WNP), PI decreases. However, the efficiency term actually increases. This increase in the efficiency term reduces the decrease in PI during CP El Niño by 10%–27%. In the case of EP and Mix El Niño over the western MDR and La Niña over the eastern MDR, the energy and the efficiency term have the same sign. Both terms negatively contribute to PI, resulting in a PI decrease. For EP and Mix El Niño over the eastern MDR, the energy term decreases while the efficiency term increases. Because the energy term still dominates, PI decreases. In short, because the efficiency

term is typically the smaller term, the contribution from efficiency is often obscured by the presence of the more dominant contribution from the energy term.

There has been considerable research done in understanding how SST changes with different climate conditions. We recommend continued improved understanding of  $T_o$  and related upper atmospheric temperatures (Emanuel et al., 2013; Kossin, 2015; Sun et al., 2024; Vecchi et al., 2013; Wing et al., 2015) under different climate conditions. We observed that  $T_o$  changes during CP El Niño, in the eastern MDR during EP/Mix El Niño, and in the western MDR during La Niña tend to follow a moist adiabatic process, that is, when the surface temperature is warm/cool, upper temperatures become warmer/cooler. In contrast, changes in  $T_o$  in the western MDR during EP and Mix El Niño events, as well as in the eastern MDR during La Niña, appear to be influenced by additional factors. For example, during the EP El Niño events in 1982, 1997, and 2023, we find that  $T_o$  in 1997 and 2023 tend to follow a moist adiabatic process, while  $T_o$  in 1982 was notably warmer (Figures S1 in Supporting Information S1). This increase in 1982 was likely influenced by the El Chichón volcanic eruption, which warmed upper atmospheric temperatures (Fujiwara et al., 2015; Randel et al., 2000; Tegtmeier et al., 2020). Additionally, other potential factors may also influence  $T_o$ , such as variability in the Brewer–Dobson circulation or changes in stratospheric ozone concentrations (Emanuel et al., 2013).

During the study period, there are many more La Niña (14 events) and CP El Niño (7 events) events than there are EP El Niño (3 events) and Mix type (3 events). We intend to refine our results further as more events are added to these two ENSO types in the future.

Several additional issues warrant further exploration. First, due to the complexity of ENSO (Capotondi et al., 2020; Timmermann et al., 2018), TC thermodynamic efficiency may vary across individual ENSO events, whether they are single- or multi-year, as well as across different ENSO phases. Secondly, we observed that the efficiency signal north of 25°N in different ENSO types is generally stronger than that observed within the MDR. Given the observed poleward migration of TCs in the WNP in recent decades (Kossin et al., 2014; Lin et al., 2023), the importance of the efficiency term contribution to PI may increase in future ENSO events. Finally, our results obtained from the reanalysis data set could be inter-compared using climate models.

### Conflict of Interest

The authors declare no conflicts of interest relevant to this study.

### Data Availability Statement

The ERA5 reanalysis data sets were obtained from the Copernicus Climate Change Service (C3S) Climate Data Store (CDS) at <https://doi.org/10.24381/cds.6860a573> (Hersbach et al., 2023a) and <https://doi.org/10.24381/cds.f17050d7> (Hersbach et al., 2023b). The original code for calculating PI can be found at Kerry Emanuel's website: <https://texmex.mit.edu/pub/emanuel/TCMAX/>. The monthly Niño-3.4 index was obtained from the National Oceanic and Atmospheric Administration (NOAA) Climate Prediction Center website at [https://www.cpc.ncep.noaa.gov/products/analysis\\_monitoring/ensostuff/ONI\\_change.shtml](https://www.cpc.ncep.noaa.gov/products/analysis_monitoring/ensostuff/ONI_change.shtml). The EP and CP indexes were taken from <https://www.ess.uci.edu/~yu/2OSC/> (Kao & Yu, 2009; J.-Y. Yu & Kim, 2010). The U.S. Joint Typhoon Warning Center (JTWC) best-track archive data is available at <https://www.metoc.navy.mil/jtwc/jtwc.html?western-pacific>.

### References

- Ashok, K., Behera, S. K., Rao, S. A., Weng, H., & Yamagata, T. (2007). El Niño Modoki and its possible teleconnection. *Journal of Geophysical Research*, 112(C11). <https://doi.org/10.1029/2006JC003798>
- Bister, M., & Emanuel, K. A. (1998). Dissipative heating and hurricane intensity. *Meteorology and Atmospheric Physics*, 65(3), 233–240. <https://doi.org/10.1007/BF01030791>
- Bister, M., & Emanuel, K. A. (2002). Low frequency variability of tropical cyclone potential intensity 1. Interannual to interdecadal variability. *Journal of Geophysical Research*, 107(D24), 4801. <https://doi.org/10.1029/2001JD000776>
- Camargo, S. J., Emanuel, K. A., & Sobel, A. H. (2007). Use of a genesis potential index to diagnose ENSO effects on tropical cyclone genesis. *Journal of Climate*, 20(19), 4819–4834. <https://doi.org/10.1175/JCLI4282.1>
- Camargo, S. J., Murakami, H., Bloemendaal, N., Chand, S. S., Deshpande, M. S., Dominguez-Sarmiento, C., et al. (2023). An update on the influence of natural climate variability and anthropogenic climate change on tropical cyclones. *Tropical Cyclone Research and Review*, 12(3), 216–239. <https://doi.org/10.1016/j.tcr.2023.10.001>
- Camargo, S. J., & Sobel, A. H. (2005). Western North Pacific tropical cyclone intensity and ENSO. *Journal of Climate*, 18(15), 2996–3006. <https://doi.org/10.1175/JCLI3457.1>

### Acknowledgments

This study is supported by the National Science and Technology Council (NSTC) of Taiwan (Grant NSTC 114-2123-M-002-003-). We thank Yen-Ting Hwang for comments during the initial phase of this work. We also sincerely thank both reviewers and the editor for their valuable suggestions.

- Capotondi, A., Wittenberg, A. T., Kug, J.-S., Takahashi, K., & McPhaden, M. J. (2020). ENSO diversity. In M. J. McPhaden, A. Santoso, & W. Cai (Eds.), *El Niño Southern Oscillation in a changing climate* (pp. 65–86). American Geophysical Union. <https://doi.org/10.1002/9781119548164.ch4>
- Chiang, J. C. H., & Sobel, A. H. (2002). Tropical tropospheric temperature variations caused by ENSO and their influence on the remote tropical climate. *Journal of Climate*, *15*(18), 2616–2631. [https://doi.org/10.1175/1520-0442\(2002\)015<2616:TTVCB>2.0.CO;2](https://doi.org/10.1175/1520-0442(2002)015<2616:TTVCB>2.0.CO;2)
- Choi, Y., Ha, K.-J., & Jin, F.-F. (2019). Seasonality and El Niño diversity in the relationship between ENSO and western North Pacific tropical cyclone activity. *Journal of Climate*, *32*(23), 8021–8045. <https://doi.org/10.1175/JCLI-D-18-0736.1>
- Chu, P.-S. (2002). Large-Scale circulation features associated with decadal variations of tropical cyclone activity over the central North Pacific. *Journal of Climate*, *15*(18), 2678–2689. [https://doi.org/10.1175/1520-0442\(2002\)015<2678:LSCFAW>2.0.CO;2](https://doi.org/10.1175/1520-0442(2002)015<2678:LSCFAW>2.0.CO;2)
- Chu, P.-S., & Murakami, H. (2022). *Climate variability and tropical cyclone activity*. Cambridge University Press. <https://doi.org/10.1017/9781108586467>
- Emanuel, K., & Rotunno, R. (2011). Self-Stratification of tropical cyclone outflow. Part I: Implications for storm structure. *Journal of the Atmospheric Sciences*, *68*(10), 2236–2249. <https://doi.org/10.1175/JAS-D-10-05024.1>
- Emanuel, K., Solomon, S., Folini, D., Davis, S., & Cagnazzo, C. (2013). Influence of tropical tropopause layer cooling on Atlantic hurricane activity. *Journal of Climate*, *26*(7), 2288–2301. <https://doi.org/10.1175/JCLI-D-12-00242.1>
- Emanuel, K. A. (1986). An air-sea interaction theory for tropical cyclones. Part I: Steady-state maintenance. *Journal of the Atmospheric Sciences*, *43*(6), 585–605. [https://doi.org/10.1175/1520-0469\(1986\)043<0585:AASITF>2.0.CO;2](https://doi.org/10.1175/1520-0469(1986)043<0585:AASITF>2.0.CO;2)
- Fujiwara, M., Hibino, T., Mehta, S. K., Gray, L., Mitchell, D., & Anstey, J. (2015). Global temperature response to the major volcanic eruptions in multiple reanalysis data sets. *Atmospheric Chemistry and Physics*, *15*(23), 13507–13518. <https://doi.org/10.5194/acp-15-13507-2015>
- Gilford, D. M. (2021). pyPI (v1.3): Tropical cyclone potential intensity calculations in python. *Geoscientific Model Development*, *14*(5), 2351–2369. <https://doi.org/10.5194/gmd-14-2351-2021>
- Gilford, D. M., Solomon, S., & Emanuel, K. A. (2017). On the seasonal cycles of tropical cyclone potential intensity. *Journal of Climate*, *30*(16), 6085–6096. <https://doi.org/10.1175/JCLI-D-16-0827.1>
- Gilford, D. M., Solomon, S., & Emanuel, K. A. (2019). Seasonal cycles of along-track tropical cyclone maximum intensity. *Monthly Weather Review*, *147*(7), 2417–2432. <https://doi.org/10.1175/MWR-D-19-0021.1>
- Ha, K.-J., Yoon, S.-J., Yun, K.-S., Kug, J.-S., Jang, Y.-S., & Chan, J. C. L. (2012). Dependency of typhoon intensity and genesis locations on El Niño phase and SST shift over the western North Pacific. *Theoretical and Applied Climatology*, *109*(3), 383–395. <https://doi.org/10.1007/s00704-012-0588-z>
- Hersbach, H., Bell, B., Berrisford, P., Biavati, G., Horányi, A., Muñoz Sabater, J., et al. (2023a). ERA5 monthly averaged data on pressure levels from 1940 to present [Dataset]. *Copernicus Climate Change Service (C3S) Climate Data Store (CDS)*. <https://doi.org/10.24381/cds.6860a573>
- Hersbach, H., Bell, B., Berrisford, P., Biavati, G., Horányi, A., Muñoz Sabater, J., et al. (2023b). ERA5 monthly averaged data on single levels from 1940 to present [Dataset]. *Copernicus Climate Change Service (C3S) Climate Data Store (CDS)*. <https://doi.org/10.24381/cds.f17050d7>
- Hersbach, H., Bell, B., Berrisford, P., Hirahara, S., Horányi, A., Muñoz-Sabater, J., et al. (2020). The ERA5 global reanalysis. *Quarterly Journal of the Royal Meteorological Society*, *146*(730), 1999–2049. <https://doi.org/10.1002/qj.3803>
- Hsu, P.-C., Chu, P.-S., Murakami, H., & Zhao, X. (2014). An abrupt decrease in the late-season typhoon activity over the western North Pacific. *Journal of Climate*, *27*(11), 4296–4312. <https://doi.org/10.1175/JCLI-D-13-00417.1>
- Huan, D., & Yan, Q. (2024). Asymmetric and irreversible response of tropical cyclone potential intensity to CO<sub>2</sub> removal. *Geophysical Research Letters*, *51*(14), e2024GL109269. <https://doi.org/10.1029/2024GL109269>
- Jin, F.-F. (1997). An equatorial ocean recharge paradigm for ENSO. Part I: Conceptual model. *Journal of the Atmospheric Sciences*, *54*(7), 811–829. [https://doi.org/10.1175/1520-0469\(1997\)054<0811:AEORPF>2.0.CO;2](https://doi.org/10.1175/1520-0469(1997)054<0811:AEORPF>2.0.CO;2)
- Kao, H.-Y., & Yu, J.-Y. (2009). Contrasting eastern-Pacific and central-Pacific types of ENSO. *Journal of Climate*, *22*(3), 615–632. <https://doi.org/10.1175/2008JCLI2309.1>
- Kim, H.-M., Webster, P. J., & Curry, J. A. (2011). Modulation of North Pacific tropical cyclone activity by three phases of ENSO. *Journal of Climate*, *24*(6), 1839–1849. <https://doi.org/10.1175/2010JCLI3939.1>
- Knutson, T. R., Chung, M. V., Vecchi, G., Sun, J., Hsieh, T.-L., & Smith, A. J. P. (2021). ScienceBrief Review: Climate change is probably increasing the intensity of tropical cyclones. In C. Le Quéré, P. Liss, & P. Forster (Eds.), *Critical issues in climate change science*. <https://doi.org/10.5281/zenodo.4570334>
- Kossin, J. P. (2015). Validating atmospheric reanalysis data using tropical cyclones as thermometers. *Bulletin of the American Meteorological Society*, *96*(7), 1089–1096. <https://doi.org/10.1175/BAMS-D-14-00180.1>
- Kossin, J. P., Emanuel, K. A., & Vecchi, G. A. (2014). The poleward migration of the location of tropical cyclone maximum intensity. *Nature*, *509*(7500), 349–352. <https://doi.org/10.1038/nature13278>
- Kug, J.-S., Jin, F.-F., & An, S.-I. (2009). Two types of El Niño events: cold tongue El Niño and warm pool El Niño. *Journal of Climate*, *22*(6), 1499–1515. <https://doi.org/10.1175/2008JCLI2624.1>
- Lee, C.-Y., Camargo, S. J., Francis, C., Karamperidou, C., & Patricola-DiRosario, C. M. (2025). Climate change impact on the ENSO-TC relationship in CMIP6: Synthetic TC analysis. *Journal of Climate*, *38*(20), 5595–5614. <https://doi.org/10.1175/JCLI-D-24-0662.1>
- Lin, I.-I., Camargo, S. J., Lien, C.-C., Shi, C.-A., & Kossin, J. P. (2023). Poleward migration as global warming’s possible self-regulator to restrain future western North Pacific Tropical Cyclone’s intensification. *npj Climate and Atmospheric Science*, *6*(1), 34. <https://doi.org/10.1038/s41612-023-00329-y>
- Lin, I.-I., Camargo, S. J., Patricola, C. M., Boucharel, J., Chand, S., Klotzbach, P., et al. (2020). ENSO and tropical cyclones. In M. J. McPhaden, A. Santoso, & W. Cai (Eds.), *El Niño Southern Oscillation in a changing climate* (pp. 377–408). American Geophysical Union. <https://doi.org/10.1002/9781119548164.ch17>
- Liu, Z., Chen, X., Sun, C., Cao, M., Wu, X., & Lu, S. (2019). Influence of ENSO events on tropical cyclone activity over the western North Pacific. *Journal of Ocean University of China*, *18*(4), 784–794. <https://doi.org/10.1007/s11802-019-3923-5>
- McPhaden, M. J., Santoso, A., & Cai, W. (2020). Introduction to El Niño Southern Oscillation in a changing climate. In M. J. McPhaden, A. Santoso, & W. Cai (Eds.), *El Niño Southern Oscillation in a changing climate* (pp. 1–19). American Geophysical Union. <https://doi.org/10.1002/9781119548164.ch1>
- Paek, H., Yu, J. Y., & Qian, C. (2017). Why were the 2015/2016 and 1997/1998 extreme El Niños different? *Geophysical Research Letters*, *44*(4), 1848–1856. <https://doi.org/10.1002/2016GL071515>
- Patricola-DiRosario, C. M., Camargo, S. J., Klotzbach, P. J., Saravanan, R., & Chang, P. (2018). The influence of ENSO flavors on western North Pacific tropical cyclone activity. *Journal of Climate*, *31*(14), 5395–5416. <https://doi.org/10.1175/JCLI-D-17-0678.1>
- Peduzzi, P., Chatenoux, B., Dao, H., De Bono, A., Herold, C., Kossin, J., et al. (2012). Global trends in tropical cyclone risk. *Nature Climate Change*, *2*(4), 289–294. <https://doi.org/10.1038/nclimate1410>

- Randel, W. J., Wu, F., & Gaffen, D. J. (2000). Interannual variability of the tropical tropopause derived from radiosonde data and NCEP reanalyses. *Journal of Geophysical Research*, *105*(D12), 15509–15523. <https://doi.org/10.1029/2000JD900155>
- Schreck, C. J., III, Knapp, K. R., & Kossin, J. P. (2014). The impact of best track discrepancies on global tropical cyclone climatologies using IBTrACS. *Monthly Weather Review*, *142*(10), 3881–3899. <https://doi.org/10.1175/MWR-D-14-00021.1>
- Shields, S., Wing, A. A., & Gilford, D. M. (2020). A global analysis of interannual variability in potential and actual tropical cyclone intensities. *Geophysical Research Letters*, *47*(18), e2020GL089512. <https://doi.org/10.1029/2020GL089512>
- Sobel, A. H., Camargo, S. J., Hall, T. M., Lee, C.-Y., Tippett, M. K., & Wing, A. A. (2016). Human influence on tropical cyclone intensity. *Science*, *353*(6296), 242–246. <https://doi.org/10.1126/science.aaf6574>
- Sobel, A. H., Lee, C.-Y., Bowen, S. G., Camargo, S. J., Cane, M. A., Clement, A., et al. (2023). Near-term tropical cyclone risk and coupled Earth system model biases. *Proceedings of the National Academy of Sciences*, *120*(33), e2209631120. <https://doi.org/10.1073/pnas.2209631120>
- Sobel, A. H., Wing, A. A., Camargo, S. J., Patricola-DiRosario, C. M., Vecchi, G. A., Lee, C.-Y., & Tippett, M. K. (2021). Tropical cyclone frequency. *Earth's Future*, *9*(12), e2021EF002275. <https://doi.org/10.1029/2021EF002275>
- Song, J., Klotzbach, P. J., & Duan, Y. (2020). Differences in western North Pacific tropical cyclone activity among three El Niño phases. *Journal of Climate*, *33*(18), 7983–8002. <https://doi.org/10.1175/JCLI-D-20-0162.1>
- Sun, Y., Feng, Z., Zhong, W., Zhai, P., Lin, Y., & Lyu, S. (2024). Uptrend of the western North Pacific tropical cyclone outflow height during 1959–2021. *Journal of Meteorological Research*, *38*(2), 339–350. <https://doi.org/10.1007/s13351-024-3097-y>
- Tegtmeier, S., Anstey, J., Davis, S., Dragani, R., Harada, Y., Ivanciu, I., et al. (2020). Temperature and tropopause characteristics from reanalyses data in the tropical tropopause layer. *Atmospheric Chemistry and Physics*, *20*(2), 753–770. <https://doi.org/10.5194/acp-20-753-2020>
- Timmermann, A., An, S.-I., Kug, J.-S., Jin, F.-F., Cai, W., Capotondi, A., et al. (2018). El Niño–Southern Oscillation complexity. *Nature*, *559*(7715), 535–545. <https://doi.org/10.1038/s41586-018-0252-6>
- Trenberth, K. E. (2020). ENSO in the global climate System. In M. J. McPhaden, A. Santoso, & W. Cai (Eds.), *El Niño Southern Oscillation in a changing climate* (pp. 21–37). American Geophysical Union. <https://doi.org/10.1002/9781119548164.ch2>
- Trenberth, K. E., Caron, J. M., Stepaniak, D. P., & Worley, S. (2002). Evolution of El Niño–Southern Oscillation and global atmospheric surface temperatures. *Journal of Geophysical Research*, *107*(D8). <https://doi.org/10.1029/2000JD000298>
- Vecchi, G. A., Fueglistaler, S., Held, I. M., Knutson, T. R., & Zhao, M. (2013). Impacts of atmospheric temperature trends on tropical cyclone activity. *Journal of Climate*, *26*(11), 3877–3891. <https://doi.org/10.1175/JCLI-D-12-00503.1>
- Wang, B., & Chan, J. C. L. (2002). How strong ENSO events affect tropical storm activity over the western North Pacific. *Journal of Climate*, *15*(13), 1643–1658. [https://doi.org/10.1175/1520-0442\(2002\)015<1643:HSEETAT>2.0.CO;2](https://doi.org/10.1175/1520-0442(2002)015<1643:HSEETAT>2.0.CO;2)
- Wang, C., Li, C., Mu, M., & Duan, W. (2013). Seasonal modulations of different impacts of two types of ENSO events on tropical cyclone activity in the western North Pacific. *Climate Dynamics*, *40*(11), 2887–2902. <https://doi.org/10.1007/s00382-012-1434-9>
- Wehner, M. F., & Kossin, J. P. (2024). The growing inadequacy of an open-ended Saffir–Simpson hurricane wind scale in a warming world. *Proceedings of the National Academy of Sciences*, *121*(7), e2308901121. <https://doi.org/10.1073/pnas.2308901121>
- Wilks, D. S. (2019). Chapter 5 - Frequentist Statistical Inference. In D. S. Wilks (Ed.), *Statistical methods in the Atmospheric sciences* (pp. 143–207). Elsevier. <https://doi.org/10.1016/B978-0-12-815823-4.00005-5>
- Wing, A. A., Emanuel, K., & Solomon, S. (2015). On the factors affecting trends and variability in tropical cyclone potential intensity. *Geophysical Research Letters*, *42*(20), 8669–8677. <https://doi.org/10.1002/2015GL066145>
- Wu, L., Zhang, H., Chen, J.-M., & Feng, T. (2018). Impact of two types of El Niño on tropical cyclones over the western North Pacific: Sensitivity to location and intensity of Pacific warming. *Journal of Climate*, *31*(5), 1725–1742. <https://doi.org/10.1175/JCLI-D-17-0298.1>
- Yu, J., Wang, Y., & Hamilton, K. (2010). Response of tropical cyclone potential intensity to a global warming scenario in the IPCC AR4 CGCMs. *Journal of Climate*, *23*(6), 1354–1373. <https://doi.org/10.1175/2009JCLI2843.1>
- Yu, J.-Y., & Kim, S. T. (2010). Three evolution patterns of Central-Pacific El Niño. *Geophysical Research Letters*, *37*(8). <https://doi.org/10.1029/2010GL042810>
- Yu, J.-Y., & Kim, S. T. (2013). Identifying the types of major El Niño events since 1870. *International Journal of Climatology*, *33*(8), 2105–2112. <https://doi.org/10.1002/joc.3575>
- Zhao, H., & Wang, C. (2019). On the relationship between ENSO and tropical cyclones in the western North Pacific during the boreal summer. *Climate Dynamics*, *52*(1), 275–288. <https://doi.org/10.1007/s00382-018-4136-0>
- Zhao, J., Zhan, R., Murakami, H., Wang, Y., Xie, S.-P., Zhang, L., & Guo, Y. (2023). Atmospheric modes fiddling the simulated ENSO impact on tropical cyclone genesis over the Northwest Pacific. *npj Climate and Atmospheric Science*, *6*(1), 213. <https://doi.org/10.1038/s41612-023-00537-6>
- Zheng, Z.-W., Lin, I.-I., Wang, B., Huang, H.-C., & Chen, C.-H. (2015). A long neglected damper in the El Niño—Typhoon relationship: A Gaia-Like process. *Scientific Reports*, *5*(1), 11103. <https://doi.org/10.1038/srep11103>